JOURNAL OF PROPULSION AND POWER
Vol. 12, No. 6, November–December 1996

Technical Notes

TECHNICAL NOTES are short manuscripts describing new developments or important results of a preliminary nature. These Notes cannot exceed 6 manuscript pages and 3 figures; a page of text may be substituted for a figure and vice versa. After informal review by the editors, they may be published within a few months of the date of receipt. Style requirements are the same as for regular contributions (see inside back cover).

Arcjet Anode Sheath Voltage Measurement by Langmuir Probe

Nicholas T. Tiliakos* and Rodney L. Burton†
University of Illinois at Urbana–Champaign, Urbana, Illinois 61801

Introduction

ELECTROTHERMAL arcjets have demonstrated higher specific impulse than conventional chemical propulsion thrusters, requiring less propellant for satellites. The achievement of high specific impulse, above 600 s for a hydrazine arcjet, requires a power-to-mass flow rate of $P/\dot{m}$ of ~80 MJ/kg, resulting in anode heating rates that can cause electrode failure. Anode heating, a critical life-limiting factor for high-performance arcjets,[1] is determined by the physics of arc attachment.[2]

One of the major contributions to anode heating is the electron power deposition in the anode sheath, as shown in Eq. (1) for a collisionless electron-repelling thin sheath[3,4]:

$$q_e = j(2kT_{es}/e + W) \tag{1}$$

For a collisionless electron-attracting thin sheath, the anode heating is[5]

$$q_e = j(5kT_{es}/2e + \phi_s + W) \tag{2}$$

where ablation, thermionic emission, Joule heating of the anode, convection, and radiation from the plasma are neglected. In Eqs. (1) and (2), $j > 0$ is the current density leaving the anode, ϕ_s is the sheath voltage, where $\phi_s > 0$ for an electron-attracting sheath and $\phi_s < 0$ for an electron-repelling sheath, T_{es} is the electron temperature at the sheath edge, and W is the work function of the 2% thoriated tungsten anode, 3.70 ± 0.85 eV.[6] For an electron-attracting sheath[7] $j \cong j_{th}$ and for an electron-repelling sheath[3] $j \cong j_{th} \exp(-|e\phi_s|/kT_{es})$, where the electron thermal current density is $j_{th} = en_{es}(kT_{es}/2\pi m_e)^{1/2}$.

There has been some confusion in the literature over the coefficient of the electron thermal energy term in Eqs. (1) and (2).[3,5] For an electron-repelling sheath Eq. (1) is derived[4] by integrating the electron kinetic energy flux over a Maxwellian distribution, with a lower limit of integration on the electron perpendicular velocity of $(2e\phi_s/m_e)^{1/2}$. For an electron-attracting sheath the electron kinetic energy flux is integrated over an anisotropic Maxwellian distribution, in which the electron perpendicular velocity is shifted by its drift velocity j/en_{es}.[5] The 5/2 factor results because all electrons in the Maxwellian distribution, not just those with velocities greater than $(2e\phi_s/m_e)^{1/2}$, enter the sheath and strike the anode. The numerical discrepancy in the limit $\phi_s \to 0$ of Eqs. (1) and (2) remains to be resolved.

Theoretical work focusing on the interaction of the sheath with the plasma bulk flow[2,8,9] has shed some light on the physics of arc attachment, but there have been no supporting experimental data on sheath characteristics for arcjets. In this Note an experiment is described in which a single miniature planar langmuir probe, flush-mounted inside an arcjet nozzle, is used to obtain both current density j and ϕ_s by directly measuring electron number density n_{es} and electron temperature T_{es} at the sheath edge. Langmuir probes have recently been used in magnetoplasmadynamic thrusters[10] and arcjet plumes[11] as a diagnostic. They are relatively simple to use and provide a convenient method of obtaining local plasma sheath properties near the probe, including arc attachment and anode heating. Such local measurements can also help to validate numerical model predictions, and guide these models to describe the near-anode physics more accurately.

Probe Measurements

A low-power arcjet, operating on simulated hydrazine and based on a standard 1-kW design,[12] was modified to accommodate a flush-mounted langmuir probe downstream of the constrictor exit in the diverging section of the nozzle. The grounded-anode conical nozzle has an area ratio of 225, a constrictor diameter of 1.0 mm, and a constrictor length of 1.5 mm. The converging cone half-angle is 30 deg, and the diverging section half-angle is 20 deg. The langmuir probe was made of 0.37-mm-diam tungsten wire, mounted flush with the end of a 0.79 mm diameter × 0.14 mm wall alumina tube. Both the probe and the insulator were positioned flush with the inner anode surface 1.7 mm downstream of the arcjet constrictor. The probe collected current on the exposed end of area $A_{pr} = 0.10$ mm^2.

The probe was biased with a single ±14.5-V, 10-Hz sinusoidal pulse, and collected probe current was measured from the voltage drop across a 100-Ω shunt resistor to generate a probe I–V_p characteristic, from which T_{es}, n_{es}, and j were obtained. Probe voltage V_p was measured with respect to the facility-grounded anode, digitally sampled at 28 kHz.

The thruster was mounted in a 1.5-m^3 vacuum tank, with a typical background pressure of ~150 mtorr, and was operated on $N_2 + 2H_2$ at 8.2 A, 101 V, 60 mg/s, and 9.5 A, 131 V, and 85 mg/s.

Experimental Results

Analysis of the probe characteristic assumes that the anode sheath is thin and collisionless, simplifying the extraction of n_{es} and T_{es} data. Calculation of the Debye length gives $\lambda_D \sim 17$ μm, verifying that the sheath is thin compared to the 380-μm-diam probe. Estimates of the electron mean-free-path λ

Received Oct. 2, 1995; revision received Feb. 16, 1996; accepted for publication April 15, 1996.

*Ph.D. Candidate, Department of Aeronautical and Astronautical Engineering, 104 South Wright Street. Student Member AIAA.

†Associate Professor, Department of Aeronautical and Astronautical Engineering, 104 South Wright Street. Associate Fellow AIAA.

for collisions with molecules give $\lambda/\lambda_D \sim 1$ at the probe location, so that electrons are approximately collisionless in the sheath. Ions, however, with a mean-free-path of $\sim 0.1\lambda_D$, are collisional in the sheath.

Probe characteristics for the two arcjet operating conditions are shown in Figs. 1 and 2, with data presented in Table 1. It is immediately evident that although the general shape of the characteristics is similar, they are shifted relative to each other in voltage. Both characteristics exhibit a knee in the curve, which occurs at the plasma potential ϕ_{pl}. The current density j is determined from the current at $V_p = 0$, when the probe and anode potential are equal. T_{es} is found from the slope of the transition region, the linear region between the floating potential ϕ_f and the plasma potential ϕ_{pl}. The electron number density is determined from the electron temperature, the electron saturation current I_e^* at ϕ_{pl} and the probe area A_{pr}[13]:

$$n_{es} = (I_e^*/eA_{pr})/\sqrt{2\pi m_e/kT_{es}}) \ (\mathrm{m}^{-3}) \tag{3}$$

The determination of sheath potential ϕ_s is discussed later.

Table 1 Experimental data for conditions of electron-repelling and electron-attracting sheaths

Sheath type	*e*-repelling, Fig. 1	*e*-attracting, Fig. 2
$\dot{m}$, mg/s	60	85
arcjet current, I, A	8.2	9.5
n_{es}, m^{-3}	$5.0 \pm 0.8 \times 10^{17}$	$7.7 \pm 1.2 \times 10^{17}$
T_{es}, K	13,300 ± 2000	10,800 ± 2000
j, A/cm^2	0.52 ± 0.08	2.2 ± 0.33
j_{th}, A/cm^2]	1.43 ± 0.2	2.0 ± 0.30
ϕ_f, V	−2.0 ± 0.4	−5.5 ± 0.4
ϕ_{pl}, V	1.6 ± 0.4	−1.7 ± 0.4
ϕ_s, V	−1.6 ± 0.4	1.7 ± 0.4

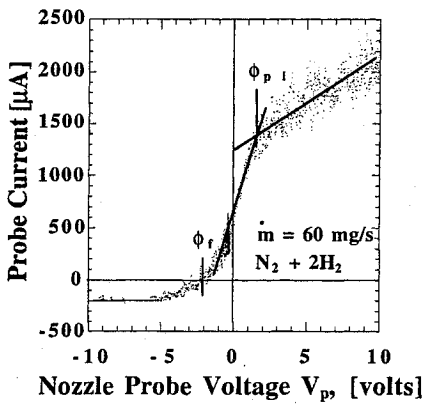

Fig. 1 Nozzle probe characteristic for an electron-repelling sheath. Arcjet conditions are $\dot{m}$ = 60 mg/s and I = 8.2 A. Probe current density at V_p = 0 is j = 0.52 A/cm^2, and plasma potential is ϕ_{pl} = 1.6 V, corresponding to ϕ_s = −1.6 V. The characteristic predicts T_{es} = 13,300 K and $n_{es} = 5.0 \times 10^{17}$ m^{-3} from the transition region $-2 < V_p < 1$ V.

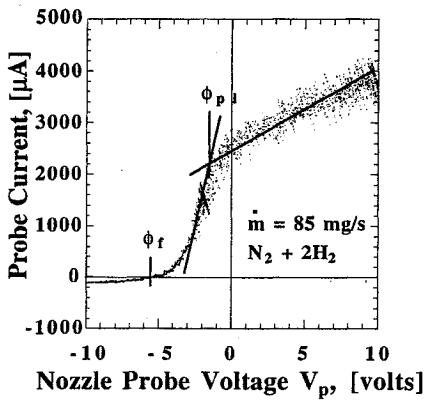

Fig. 2 Nozzle probe characteristic for an electron-attracting sheath. Arcjet conditions are $\dot{m}$ = 85 mg/s and I = 9.5 A. Probe current density at V_p = 0 is j = 2.2 A/cm^2, and plasma potential is ϕ_{pl} = −1.7 V, corresponding to ϕ_s = 1.7 V. The characteristic predicts T_{es} = 10,800 K and $n_{es} = 7.7 \times 10^{17}$ m^{-3} from the transition region $-4 < V_p < -2.5$ V.

Sheath Analysis

The probe I–V_p characteristic and resulting plasma properties yield three independent approaches for calculating the total sheath voltage drop ϕ_s:

1) The sheath voltage drop can be determined from the plasma potential at the knee of the characteristic from $\phi_s = -\phi_{pl}$ (see Table 1).

2) The sheath voltage drop can be determined from j and j_{th}. For electron-repelling sheaths, which occur at low values of j and high j_{th}, the anode current balance can be written[3]

$$j = j_{th} \exp(-|e\phi_s|/kT_{es}) - j_{emit} - j_{th}^i \tag{4}$$

where j_{th} and j_{th}^i are the electron and ion random thermal current densities, and j_{emit} is the current density of electrons thermionically emitted from the anode. For $T_i \approx T_{anode} < 1400$ K, the ion and emitted-electron contributions can be neglected, giving for the potential drop of an electron-repelling sheath:

$$\phi_s = (kT_{es}/e)\ell n(j/j_{th}) < 0 \tag{5}$$

Deriving n_{es}, T_{es}, j, and j_{th} from the probe characteristic, ϕ_s can be calculated from Eq. (5).

3) The sheath voltage drop can be determined from the floating potential. The current density to a probe at a potential V_p is

$$j = j_{th} \exp[e(V_p - \phi_{pl})/kT_{es}] - j_{th}^i \tag{6}$$

For $j = 0$ at $V_p = \phi_f$, with $\phi_s = -\phi_{pl}$, Eq. (6) gives

$$\phi_s = -\phi_f - (kT_{es}/e)\ell n(T_{es}M_i/T_i m_e)^{1/2} \tag{7}$$

The calculated ϕ_s values from the three methods are shown in Table 2, for $T_i \sim T_a = 1400$ K and H^+ ions.

Analysis and Conclusions

The contribution to anode heating from the current can be evaluated with Eqs. (1) and (2), using the experimental data in Table 1. For the electron-repelling sheath q_e = 3.1 W/cm^2 and for the electron-attracting sheath q_e = 14.4 W/cm^2. The

Table 2 Calculated anode sheath potentials derived from probe characteristic data

Sheath type	*e*-repelling	*e*-attracting
$\dot{m}$, mg/s	60	85
ϕ_s from knee in probe characteristic	−1.6 ± 0.4 V	+1.7 ± 0.4 V
ϕ_s from current equation [Eq. (5)], *e*-repelling sheath	−1.2 ± 0.14 V	N/A
ϕ_s from floating potential [Eq. (7)]	−3.6 ± 0.4 V	+1.1 ± 0.4 V

heating for an electron-attracting anode sheath is significantly higher than for an electron-repelling sheath, as would be expected from the higher current density. Defining an effective sheath potential as $\phi_{\text{eff}} \equiv q_e/j$ gives a similar value for the electron-repelling and electron-attracting sheaths in this experiment of $\phi_{\text{eff}} \sim 6.2 \pm 0.3$ V.

Langmuir probe measurements of an arcjet anode sheath show that the sheath potential drop can be of order 1–3 V positive or negative. The data suggest that the most significant factor in determining the sign of the potential is the anode current density, implying a critical current density for which $\phi_s = 0$. Here, $j_{\text{crit}} \sim 1$ A/cm^2.

In summary, a simple method of implementing langmuir probes has been presented that can provide direct measurements of n_{es}, T_{es}, j, and ϕ_s. Of the three methods outlined, determining ϕ_s from the plasma potential is the most reliable, since it is based on a direct measurement. Finally, as current density varies, the sheath voltage can change sign, and the arcjet anode heating can be represented by an effective potential $\phi_{\text{eff}} \sim 6.2$ V at the probe location used.

Acknowledgments

We gratefully acknowledge illuminating discussions with H. Krier and M. Kushner and critical assistance from W. Johnson, K. Elam, and J. Frizzell of the University of Illinois; support from T. Haag and J. Sankovic of NASA Lewis Research Center; Graduate Students S. Bufton and G. Willmes for assistance in the laboratory; and helpful suggestions from M. Cappelli of Stanford University. The authors acknowledge support by the U.S. Air Force Office of Scientific Research under Contracts F49620-92-J-0448 and -0280. Mitat Birkan is the Program Monitor.

References

[1]Lichon, P., and Sankovic, J., "Development and Demonstration of a 600 Second Mission Average Arcjet," 23rd International Electric Propulsion Conf., Paper 93-087, Sept. 1993.

[2]Meeks, E., and Cappelli, M. A., "A Multi-Fluid Model of Near-Electrode Plasma Behavior," AIAA Paper 93-2103, June 1993.

[3]Merinov, N. S., and Petrosov, V. A., "Existence Region for Arcing Conditions with Negative Anode Potential Drop," *Journal of Applied Mechanics and Technical Physics*, Vol. 17, No. 1, 1976, pp. 12–18.

[4]Diamant, K. D., private communication, Princeton Univ., Princeton, NJ, Oct. 1995.

[5]Oberth, R. C., "Anode Phenomena in High-Current Discharges," Ph.D. Dissertation, Dept. of Mechanical and Aerospace Engineering, Princeton Univ., Princeton, NJ, 1970.

[6]Goodfellow, K. D., and Polk, J. E., "Experimental Verification of a High-Current Cathode Thermal Model," AIAA Paper 95-3062, July 1995.

[7]Vainberg, L. I., Lyubimov, G. A., and Smolin, G. G., "High-Current Discharge Effects and Anode Damage in an End-Fire Plasma Accelerator," *Soviet Physics—Technical Physics*, Vol. 23, No. 4, 1978, pp. 439–443.

[8]Dinulescu, H. A., and Pfender, E., "Analysis of the Anode Boundary Layer of High Intensity Arcs," *Journal of Applied Physics*, Vol. 51, No. 6, 1980, pp. 3149–3157.

[9]Cappelli, M. A., "Modeling of the Near-Electrode Regions of Arcjets I: Coupling of the Flowfield to the Non-Equilibrium Boundary Layer," AIAA Paper 92-3109, July 1992.

[10]Soulas, G. C., and Myers, R. M., "Mechanisms of Anode Power Deposition in a Low Pressure Free Burning Arc," 23rd International Electric Propulsion Conf., NASA CR 194442, International Electric Propulsion Conf., Paper 93-194, Sept. 1993.

[11]Carney, L. M., and Keith, T. G., "Langmuir Probe Measurements of an Arcjet Exhaust," *Journal of Propulsion and Power*, Vol. 5, No. 3, 1989, pp. 287–293.

[12]Curran, F. M., and Haag, T. W., "An Extended Life and Performance Test of a Low Power Arcjet," AIAA Paper 88-3106, July 1988.

[13]Schott, L., "Electric Probes," *Plasma Diagnostics*, edited by W. Lochte-Holtgreven, Wiley, New York, 1968, pp. 668–731.

Application of the k-ω Turbulence Model to Quasi-Three-Dimensional Turbomachinery Flows

Rodrick V. Chima*
NASA Lewis Research Center, Cleveland, Ohio 44135

Introduction

MANY computational fluid dynamics codes for turbomachinery use the Baldwin–Lomax (B–L) turbulence model.[1] It is easy to implement in two dimensions and works well for predicting overall turbomachinery performance. However, it is awkward to implement in three dimensions, often has difficulty finding the length scale, has a crude transition model, and neglects freestream turbulence, surface roughness, and mass injection.

The k-ω model developed by Wilcox[2] is an appealing alternative for several reasons. First, it is the only two-equation model that can be integrated to the wall without requiring damping functions or the distance to the wall, and hence, should behave well numerically. Second, the effects of freestream turbulence, surface roughness, and mass injection are easily included in the model. Finally, transition can be simulated using the low Reynolds number version of the model.[3]

Menter applied the k-ω model to external flows and showed very good results for flows with adverse pressure gradients.[4] Liu and Zheng[5] described their implementation of the k-ω model in a cascade code that included an area change term to account for endwall convergence. They validated the model for a flat plate, and compared the B–L and k-ω models to measured surface pressures for a low-pressure turbine cascade. Since they did not use the low Reynolds number version of the model, their results showed problems resulting from early transition.

In this Note the low Reynolds number k-ω model was incorporated in the author's quasi-three-dimensional turbomachinery analysis code.[6] The code includes the effects of rotation, radius change, and stream-surface thickness variation, and also includes the B–L turbulence model. The k-ω model was implemented using many of Menter's[4] recommendations and an implicit approximate-factorization scheme described by Baldwin and Barth.[7] The model was tested for a transonic compressor with rotation and variable stream-surface radius and height, and for a transonic turbine vane with transition and heat transfer. Results were compared to the B–L model and to experimental data.

Quasi-Three-Dimensional Navier–Stokes Code

The quasi-three-dimensional Navier–Stokes equations have been developed for an axisymmetric stream surface in an (m, θ) coordinate system as shown in Fig. 1. The meridional coordinate m is given by $dm^2 = dz^2 + dr^2$, and the tangential coordinate θ rotates with the blade row with angular velocity Θ. The radius r and the thickness h of the stream surface are assumed to be known functions of m. The equations were mapped to a body-fitted coordinate system, nondimensional-

Received Nov. 27, 1995; presented as Paper 96-0248 at the AIAA 34th Aerospace Sciences Meeting and Exhibit, Reno, NV, Jan. 15–19, 1996; revision received May 27, 1996; accepted for publication May 28, 1996.

*Aerospace Engineer, M/S 77-6, Brookpark Road. Associate Fellow AIAA.